Appl. Phys. A (2016) 122:52
DOI 10.1007/s00339-015-9589-y

Applied Physics A
Materials Science & Processing

CrossMark

Large arrays of ultra-high aspect ratio periodic silicon nanowires obtained via top–down route

Halldor Gudfinnur Svavarsson[1] · Birgir Hrafn Hallgrimsson[1] · Manoj Niraula[2] · Kyu Jin Lee[2] · Robert Magnusson[2]

Received: 27 December 2015 / Accepted: 28 December 2015 / Published online: 11 January 2016
© Springer-Verlag Berlin Heidelberg 2016

Abstract Metal-catalysed etching (MCE) is a simple and versatile method for fabrication of silicon nanowires, of high structural quality. When combined with laser interference lithography (LIL), large areas of periodic structures can be generated in only few steps. The aspect ratio of such periodic structure is however commonly not higher than several decades or very few hundred. Here, a combined MCE and LIL techniques were applied to fabricate dense (4×10^8 cm^{-3}), periodic arrays of vertically aligned silicon nanowires with aspect ratio of up to 10^3. This is a considerable higher number than previously reported on for periodic silicon wire arrays prepared with top–down approaches. The wires were slightly tapered, with top and bottom diameters ranging from 370 to 195 nm and length of up to 200 µm. A potential use of the nanowires as light absorber is demonstrated by measuring reflection in integrating sphere. An average total absorption of ~97 % was observed for 200-µm-long wires in the spectral range of 450–1000 nm. A comparison to simulated absorption spectra is given.

1 Introduction

Low-dimensional silicon structures, such as silicon nanowires (SiNWs), have attracted large attention as a promising material for chemical and biological sensing and advanced energy conversion [1, 2]. For solar energy conversion, arrays of ordered SiNWs have been shown to provide an excellent light trapping by way of increasing the path length of incoming light, leading to suppressed optical reflection and strong broadband optical absorption [3, 4]. This feature is particularly important for solar thermal collectors and for photovoltaic (PV) devices [5]. For sensing application, like in surface-enhanced Raman spectroscopy (SERS), SiNWs with high aspect ratio have demonstrated exceptionally high SERS signal intensity due to their larger effective surface. It has also been shown that well-ordered SiNWs exhibit higher intensity and better uniformity of the SERS signal than randomly arranged SiNW [6].

Possible fabrication routes of NWs can be divided into two major categories depending on the nature of the process: a bottom-up approach in which a nucleation of crystal growth is triggered on top of an arbitrary substrate and a top–down approach in which a bulk material is etched down by a physical or chemical means. An inexpensive and versatile version of the top–down approach, metal-catalysed etching (MCE) [7], has been used efficiently to fabricate SiNWs of high structural quality [8, 9]. The technique involves highly anisotropic electrochemical etching with the aid of a catalytic metal. In a water-based solution of hydrofluoric acid (HF) and an oxidizer (typically H_2O_2), a catalysed etching of a bulk Si wafer occurs in the vicinity of the metal catalyst. The best-known catalysts are gold (Au) and silver (Ag). When used in conjunction with laser interference lithography (LIL) [10], MCE is capable of yielding densely packed periodic arrays of high aspect ratio SiNWs with tunable dimensions. Furthermore, LIL is a maskless lithography technique capable of wafer-scale patterning with dimensions down to few tens of nanometres. Many authors have reported on randomly

✉ Halldor Gudfinnur Svavarsson
halldorsv@ru.is

[1] School of Science and Engineering, Reykjavík University, 101 Reykjavík, Iceland

[2] Department of Electrical Engineering, The University of Texas at Arlington, Box 19016, Arlington, TX 76019, USA

distributed high aspect ratio wires prepared with catalytic nano-size metal particles spread over Si surface in an etchant solution. The wires had diameter typically in the range of few tens to few hundred nanometres and aspect ratio of up to roughly three orders of magnitude [11–13]. These wires, however, lack the periodicity provided by a continuous catalytic metal film as in our case, and their diameters are not either homogeneous. A continuous catalytic metal film, as obtained by LIL, is not able to sink as fast into the Si surface as does individual nano-size particles. Consequently, periodic SiNWs fabricated by LIL have not reached as high aspect ratio as wires fabricated by catalytic nano-size particles. An example of other top–down method, capable of giving periodic structure, is reactive ion etching which has given wires with diameter ranging from sub-100 nm to few µm and aspect ratio of up to roughly two orders of magnitude [14–16]. Use of block copolymer lithography and MCE has also been used to produce periodic wire arrays with aspect ratio of 220 [17].

In this paper, MCE and LIL were applied in conjunction to fabricate periodic arrays of SiNWs with homogenous diameters and aspect ratio of up to roughly three orders of magnitude. A possible application of the wires as light absorber is demonstrated.

2 Experimental part

A 2″ single-crystalline p-type (100) Si wafer with resistivity 0.01–0.05 Ωm was spin coated with positive photoresist (PR). The wafer was exposed to an interference pattern from a continuous-wave laser system with a wavelength of $\lambda = 266$ nm. The periodicity Λ of the PR pattern is given by $\Lambda = \lambda/2\sin\theta$ where λ is the wavelength and θ is the incidence angle of the incoming light. With visible light absorption in mind, a periodicity of 500 nm was chosen for this experiment. Two-dimensional PR arrays were achieved through two perpendicular exposures and subsequent removal of the exposed PR by MF-26A developer solution. On each Si wafer, either 4 × 4 array, each one being 5 × 5 mm^2 in size or 3 × 3 arrays of 5 × 5 mm^2, was prepared. The catalytic metal film was made of Au: roughly 25-nm-thick Au film was deposited on top of the nanopatterned PR with electron-beam evaporation. The effect of the catalytic film thickness has been reported to be critical, a minimum of 6 nm is required to form the wires, and increased thicknesses (up to 15 nm at least) results in less porosity of the wire's surfaces [18]. A preliminary study (not published here) had revealed that it was not possible to fabricate wires longer than few hundred nanometres when using very thin (6–10 nm) Au film. Apparently, this was because the film was exhausted after extended time (several hours) in the etching solution (as partially confirmed with X-ray measurement). A sufficient film thickness is thus needed to obtain wires with ultra-high aspect ratio in order for the film to survive extended time in the etchant. The deposition step was followed by lift-off in aqueous ma-R 404S (from Micro Resist Technology GmBh), leaving a gold mesh on top of the wafer. Prior to the Au deposition, native oxide was removed from the PR-patterned Si wafer by immersing it in 2.5 M HF solution (8 % w/w HF) in order to improve the Au/wafer adhesion. The last step in the NWs fabrication was placing the sample in HF:H_2O_2 solution. Concentration of 5 M [HF] and 0.4 M [H_2O_2] was chosen but similar concentration has been shown to be optimum for rapid generation of high aspect ratio Si nanostructures [19]. The samples were kept in the etching solution for various time intervals, ranging from 7 min to 25 h. For the longer etching time (roughly an hour or more), the samples had tendency to float up in the etching solution due to formation of gas bubbles that adhered to the nanopattern being created. This was prevented by keeping the sampling down by a plastic clamp. The etching was terminated by immersing the sample in deionized (DI) water, followed by drying with N_2 gas. Afterwards, the gold film was removed in aqueous TFA gold remover solution (from Transene Co., Inc.) and then rinsed in DI water and dried with N_2 gas. The wire length and diameters were derived from top-view and cross-view images taken with a scanning electron microscope (SEM).

Reflectance spectroscopy in the wavelength interval of λ = 500–1000 nm was applied to measure the optical reflection of transverse magnetic (TM) and transverse electric (TE) polarized light. A Koheras SuperK Compact light source with output spectrum in the range of 500–1000 nm was used. A reference signal was obtained from a silver mirror. An iris diaphragm was used to align the reflected-beam paths of the SiNWs and the silver mirror. Zeroth-order reflectance (R_0) for normal incidence was detected by Ocean Optics USB4000 optical spectrum analyser capable of covering the 350–1050-nm spectrum.

In order to account for higher order diffraction, the total absorption of unpolarized light was measured in an integrating sphere in the spectral range of 450–1000 nm using an Ocean Optics HL-2000 halogen light source and Ocean Optics USB4000 optical spectrum analyser. To assure that the zero-order reflection would be trapped within the sphere, the sample was placed at slightly off-normal incidence (roughly 8 degrees). A schematic of the set-up is shown in Fig. 1. Since no transmission was observed and all reflection is accounted for in the integrating sphere, the total absorption is defined the same way as extinction by $\frac{I_{ref}-I_{meas}}{I_{ref}}$ where I_{ref} is the intensity of the input light into the sphere measured through light output aperture in the absence of a sample and I_{meas} is the intensity of the

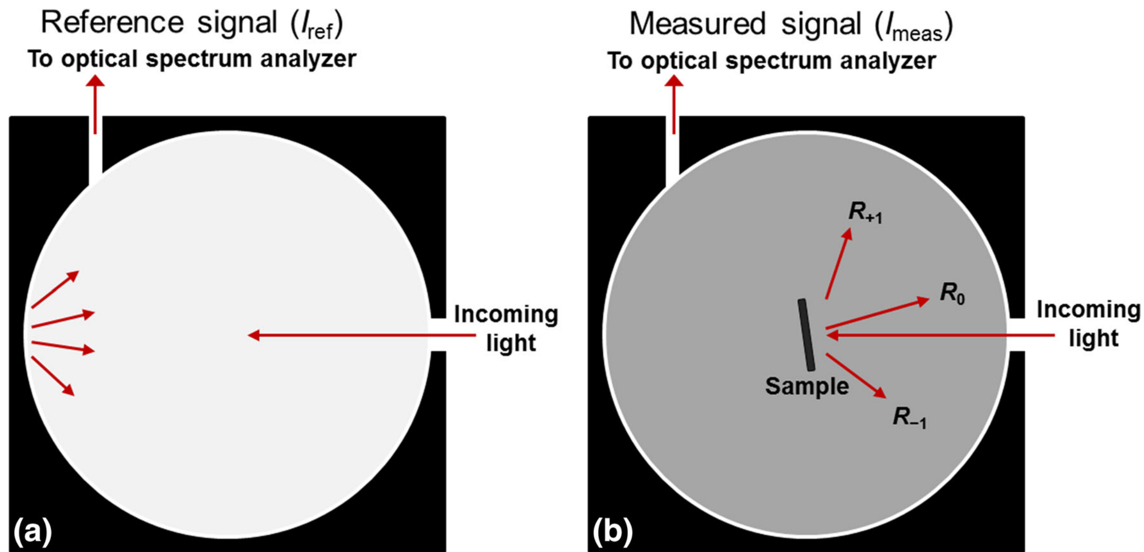

Fig. 1 Schematic of the integration-sphere set-up. Reference signal is obtained by measuring the light intensity out of the sphere in the absence of a sample (**a**). Measured signal is obtained by measuring the light intensity out of the sphere in the presence of a sample (**b**)

reflected light in the presence of a sample. The beam spot size for the reflectance measurements was 2 mm, but for the total absorption measurement, it was decreased to 1 mm with a focusing lens in order to eliminate any stray light inside the sphere.

A comparison to a numerical simulation of the absorption spectrum using commercial code RSoft DiffractMOD is given (http://www.rsoftdesign.com/). Further comparison is provided to absorption spectra for a bare Si wafer and a gold-coated wafer.

3 Results and discussion

Cross-sectional and top-view SEM images of the fabricated SiNWs are shown in Fig. 2. For the shortest etching time, 7 min (Fig. 2a), a highly regular structure is seen and the wires are vertically aligned. After 40-min etching (Fig. 2b), the periodicity as seen from the top is still quite apparent but the wires start to bend in localized areas and form bundles. After 60-min etching (Fig. 2c), the top-view periodicity has disappeared and all wires have formed bundles of roughly 10–15-μm^2 size. Similar but more pronounced phenomena are seen after 25-h etching (Fig. 2d). The bundles are likely formed due to capillary forces created upon drying the samples after etching coupled with the high surface energy of silicon.

Table 1 shows the length and diameters of the SiNWs for different etching time. The wires are slightly tapered, and therefore, two distinct values are displayed in the table: one denoting the diameter close to the top of the wires and a second one denoting the diameter at their bottom. The aspect ratio is calculated for the average of the two diameters.

Results of normalized zero-order reflectance measurements for normal incidence in the range of 500 to 1000 nm are shown in Fig. 3, left and right, for TM and TE polarized light, respectively. The graphs shown in the figures are average of measurements gotten from 4, 3, 2 and two different positions of the incoming light for the 7 min, 40 min, 60 min and 25-h samples, respectively. This was carried out to minimize the influence of possible structural perturbation. Zero (below the detection limit) transmission was observed for all samples.

As seen, the reflection is low in all cases and decreases as the wires get longer. An average reflection of < 5 % was observed over the measured wavelength range for the array with shortest wires (green line) for both TM and TE polarized lights. The reflection of the array with the longest wires was close to zero (below the detection limit) and thus not shown in the graph. We note that for the perfectly periodic array with 1.5-µm-long posts, the reflectance data are nearly the same for TE and TM polarization states as expected due to the fact that both orthogonal states experience the same structure.

Figure 4 shows the total absorption spectra of unpolarized light provided by the SiNWs arrays (left) and concomitant simulated spectra obtained with rigorous numerical electromagnetic simulations accounting for the complex, dispersive refractive index of the wires (right). The parameters of the wire's geometry used in the simulation were taken from Table 1, and the sampling resolution was 1 nm. In the simulation, the wires were taken to be perfectly periodic and vertically aligned.

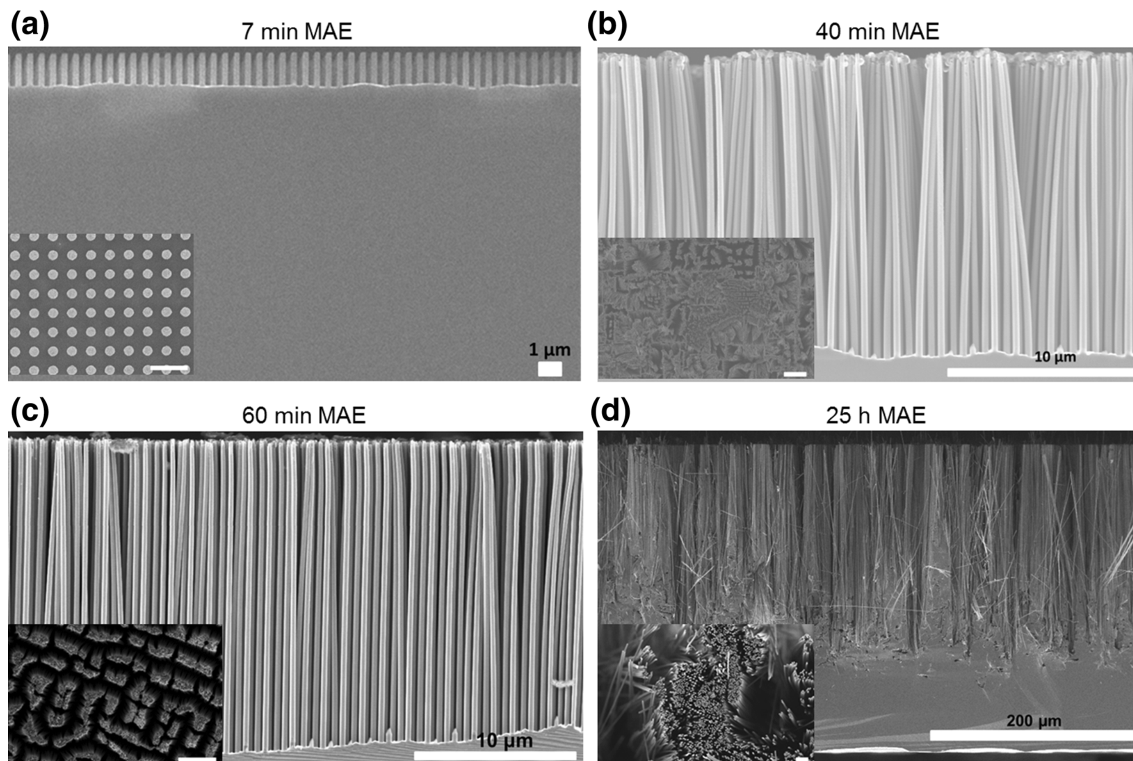

Fig. 2 Cross-sectional SEM images of silicon nanowires obtained after different etching time. The insets in the lower left corners show top views, visualizing less apparent periodicity as the wires gets longer. The scale bars on the insets are 1, 10, 10 and 2 µm for **a**, **b**, **c** and **d**, respectively

Table 1 Geometry of the fabricated SiNWs for various etching time

Parameter	Etching time			
	7 min	40 min	60 min	25 h
Upper wire diameter (nm)	300	275	265	195
Lower wire diameter (nm)	320	370	370	~300
Length (µm)	1.5	16	20	200
Average aspect ratio	5	50	63	808

Table 2 shows the average reflection and average total absorbance over the measured wavelength range of 500–1000 and 450–1000 nm, respectively. A comparison to values obtained from the simulated absorption spectrum of 450–1000 nm is given. An average total absorption of 64.9 and 14.4 % was measured for the flat Si and Au surfaces, respectively. The highest absorption is obtained for the longest wire array, 96.7 %, but a still higher value of 97.9 % is observed over the range of 500–700 nm. As

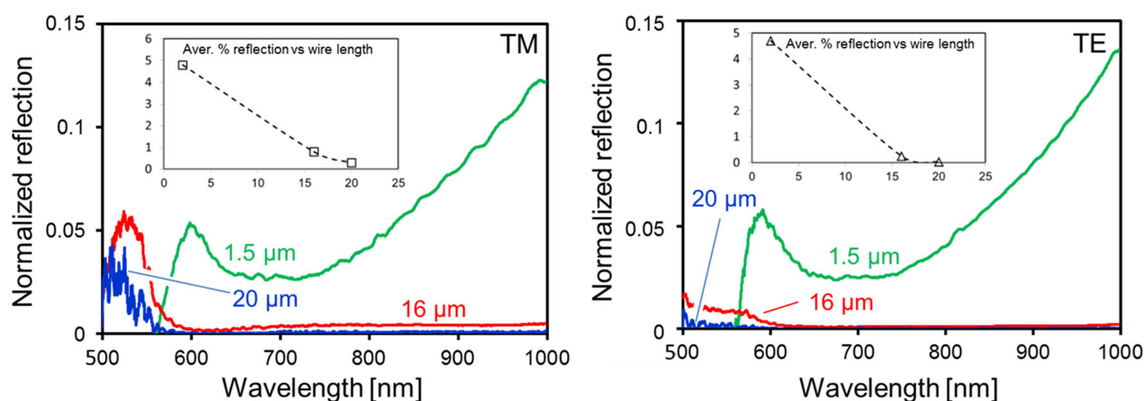

Fig. 3 Normalized reflection spectrums for normally incident light for nanowires of length 1.5 µm (*green line*), 16 µm (*red line*) and 20 µm (*blue line*). The reflection of the 25-h-etched sample was below detection limit. *Left* TM polarized light. *Right* TE polarized light. The *insets* show the average reflection over $\lambda = 500$–1000 nm in percentage versus length of the wires in micrometre

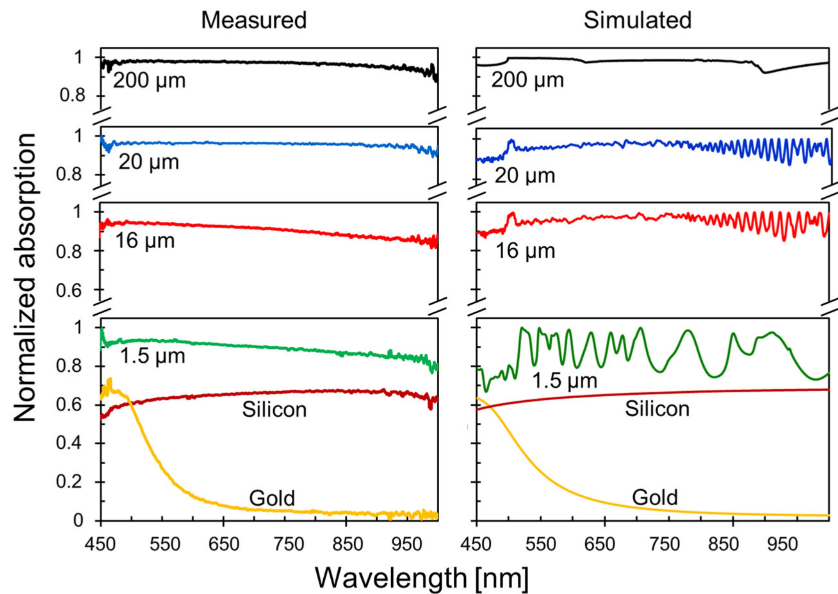

Fig. 4 Measured (*left*) and simulated (*right*) total absorption spectrum of SiNWs of length 1.5 µm (*green line*), 16 µm (*red line*), 20 µm (*blue line*) and 200 µm (*black line*). Measured spectrum from flat silicon and gold surfaces is shown for a comparison

Table 2 SiNW's average reflection of 500–1000 nm and average total absorption of 450–1000 nm

Parameter (%)	Wire length (µm)			
	1.5	16	20	200
TM reflected light	4.7	0.25	0.03	~0
TE reflected light	4.8	0.8	0.3	~0
Measured absorption	89.0	90.3	95.7	96.7
Simulated absorption	86.1	95.3	95.6	97.6

seen from the table and Fig. 4, the measured total absorption values and the simulated ones agree rather well. The largest discrepancy is seen for the 16-µm-long wires where the measured and calculated values are 90.3 and 95.3 %, respectively. From the SEM micrographs in Fig. 2, it is apparent that the wires start to bend and form bundles at roughly 16 µm length (40 min etching) and at 20 µm (60 min etching) and no periodicity is seen from the top-view micrograph.

In a recent experimental and theoretical study on optical properties of vertical high aspect ratio SiNWs [20], the light reflection was found to decrease when moving from perfectly periodic to a defective and quasi-ordered structure. It was also observed that smaller diameter and increased length of the wires decreased the reflection. A total reflectance of less than 2 % was observed for array of 4.6-µm-long and 180-nm-wide wires of period 1 µm in a wide range (~40 %) of the measured 250–1000-nm spectrum. The reflection of array of equally long wires with a diameter of 300–400 nm was three times higher. Our experimental results agree qualitatively with this study. The arrays start to deviate from periodic to quasi-periodic order at wire length of ~16 µm. It is further seen from the absorption measurements (Table 2) that the absorption of 20-µm-long wires, where quasi-periodicity prevails, is significantly higher than of the 16-µm arrays. The enhancement is more than that could be expected on the basis of the increased wire's length alone. However, the simulated spectrum which assumes perfect periodicity shows very similar absorption for the 16- and 20-µm arrays (95.3 vs. 95.6 %, respectively). In a study where rigorous coupled-wave analysis was applied to calculate the optimum dimensions of SiNWs, it was found that almost unity absorption could be obtained from a square array of 20-µm-long and 400-nm-wide Si wires [21] which is close to our geometry. The effect of our tapered structures should also increase the optical absorption by giving a graded refractive index profile at the surface; details of this effect are beyond the scope of this study.

4 Conclusion

In summary, large arrays of periodic SiNWs with ultra-high aspect ratios were fabricated with a combined use of LIL and MCE. An aspect ratio of roughly 10^3 was accomplished. An average total absorption of roughly 96 % was observed for arrays of 20-µm-long wires. Increased length in excess of that resulted, however, in only insignificant absorption enhancement.

Both MCE and LIL are suitable for large-scale patterning, and MCE in particular is an inexpensive technology. We note that the MCE technique is reported to be both suitable for single-crystalline and polycrystalline Si [22]. This is particularly important in thin-film applications

where there are normally polycrystalline or amorphous structures but rarely single-crystalline films.

It is interesting to note the agreement between the experimental data and the numerical results in Fig. 4. The agreement is quantitatively quite good even though the theoretical model assumes strict 2D periodicity. This implies that the internal order of the NW arrays is maintained on a macroscopic scale in an average sense in the experiments performed here.

Acknowledgments This research was supported in part by the Energy Research Fund of the National Power Company of Iceland and by the UT System Texas Nanoelectronics Research Superiority Award funded by the State of Texas Emerging Technology Fund. Additional support was provided by the Texas Instruments Distinguished University Chair in Nanoelectronics endowment.

Compliance with ethical standards

Conflict of interest The authors declare that they have no conflict of interest in addition to what is described in the Acknowledgments.

References

1. K. Peng, X. Wang, L. Li, Y. Hu, S. Lee, Silicon nanowires for advanced energy conversion. Nano Today **8**(1), 75–97 (2013). doi:10.1016/j.nantod.2012.12.009
2. Y. Wang, T. Wang, P. Da, M. Xu, H. Wu, G. Zheng, Silicon nanowires for biosensing, energy storage, and conversion. Adv. Mater. **25**(37), 5177–5195 (2013). doi:10.1002/adma.201301943
3. Z. Guo, J.Z.K. Jung, Y. Xiao, S. Jee, S. Moiz, J. Lee, Optical properties of silicon nanowires array fabricated by metal-assisted electroless etching. Proc. SPIE (2010). doi:10.1117/12.860397
4. M. Hasan, M. Huq, Z. Mahmood, A review on electronic and optical properties of silicon nanowire and its different growth techniques. Springerplus (2013). doi:10.1186/2193-1801-2-151
5. L. Tsakalakos, J. Balch, J. Fronheiser, B. Korevaar, O. Sulima, J. Rand, Silicon nanowire solar cells. Appl. Phys. Lett. **91**(23), 233117 (2007). doi:10.1063/1.2821113
6. J. Yang, J. Li, Q. Gong, J. Teng, M. Hong, High aspect ratio SiNW arrays with Ag nanoparticles decoration for strong SERS detection. Nanotechnology **25**(46), 465707 (2014). doi:10.1088/0957-4484/25/46/465707
7. E. Garnett, P. Yang, Light trapping in silicon nanowire solar cells. Nano Lett. **10**(3), 1082–1087 (2010). doi:10.1021/nl100161z
8. X. Li, P. Bohn, Metal-assisted chemical etching in HF/H(2)O(2) produces porous silicon. Appl. Phys. Lett. **77**(16), 2572–2574 (2000). doi:10.1063/1.1319191
9. Z. Huang, N. Geyer, P. Werner, J. de Boor, U. Gosele, Metal-assisted chemical etching of silicon: a review. Adv. Mater. **23**(2), 285–308 (2011). doi:10.1002/adma.201001784
10. J. Seo, J. Park, S. Kim, B. Park, Z. Ma, J. Choi, B. Ju, Nanopatterning by laser interference lithography: applications to optical devices. J. Nanosci. Nanotechnol. **14**(2), 1521–1532 (2014). doi:10.1166/jnn.2014.9199
11. Y. Liu, W. Sun, Y. Jiang, X. Zhao, Fabrication of bifacial wafer-scale silicon nanowire arrays with ultra-high aspect ratio through controllable metal-assisted chemical etching. Mater. Lett. **139**, 437–442 (2015). doi:10.1016/j.matlet.2014.10.084
12. M. Zaremba-Tymieniecki, C. Li, K. Fobelets, Z. Durrani, Field-effect transistors using silicon nanowires prepared by electroless chemical etching. IEEE Electron. Dev. Lett. **31**(8), 860–862 (2010). doi:10.1109/LED.2010.2050572
13. X. Li, Metal assisted chemical etching for high aspect ratio nanostructures: a review. Curr. Opin. Solid State Mater. Sci. **16**(2), 71–81 (2012). doi:10.1016/j.cossms.2011.11.002
14. A. Zeniou, K. Ellinas, A. Olziersky, E. Gogolides, Ultra-high aspect ratio Si nanowires fabricated with plasma etching: plasma processing, mechanical stability analysis against adhesion and capillary forces and oleophobicity. Nanotechnology (2010). doi:10.1088/0957-4484/25/3/035302
15. J. Nakamura, K. Higuchi, K. Maenaka, Vertical Si nanowire with ultra-high-aspect-ratio by combined top–down processing technique. Microsyst. Technol. **19**(3), 433–438 (2013). doi:10.1007/s00542-012-1662-2
16. M. Poudineh, Z. Sanaee, A. Gholizadeh, S. Soleimani, S. Mohajerzadeh, Formation of highly ordered silicon nanowires by a high-speed deep etching. IEEE Trans. Nanotechnol. **12**(5), 712–718 (2013). doi:10.1109/TNANO.2013.2269479
17. S. Chang, V. Chuang, S. Boles, C. Ross, C. Thompson, Densely packed arrays of ultra-high-aspect-ratio silicon nanowires fabricated using block-copolymer lithography and metal-assisted etching. Adv. Funct. Mater. **19**(15), 2495–2500 (2009). doi:10.1002/adfm.200900181
18. M. Lajvardi, H. Eshghi, M. Ghazi, M. Izadifard, A. Goodarzi, Structural and optical properties of silicon nanowires synthesized by Ag-assisted chemical etching. Mater. Sci. Semicond. Process. **40**, 556–563 (2015). doi:10.1016/j.mssp.2015.07.032
19. J. Ho, Q. Wee, J. Dumond, A. Tay, S. Chua, Versatile pattern generation of periodic, high aspect ratio Si nanostructure arrays with sub-50-nm resolution on a wafer scale. Nanoscale Res. Lett. (2013). doi:10.1186/1556-276X-8-506
20. A. Smyrnakis, V. Almpanis, N. Papanikolaou, V. Constantoudis, N. Papanikolaou, E. Gogolides, Optical properties of high aspect ratio plasma etched silicon nanowires: fabrication-induced variability dramatically reduces reflectance. Nanotechnology **26**(8), 085301 (2015). doi:10.1088/0957-4484/26/8/085301
21. H. Alaeian, A. Atre, J. Dionne, Optimized light absorption in Si wire array solar cells. J. Opt. **14**(2), 024006 (2012). doi:10.1088/2040-8978/14/2/024006
22. S. Chang, V. Chuang, S. Boles, C. Thompson, Metal-catalyzed etching of vertically aligned polysilicon and amorphous silicon nanowire arrays by etching direction confinement. Adv. Funct. Mater. **20**(24), 4364–4370 (2010). doi:10.1002/adfm.201000437